

THE OXYGEN FUGACITY-TEMPERATURE RELATIONSHIPS OF MANGANESE OXIDE AND NICKEL OXIDE BUFFERS¹J. STEPHEN HUEBNER AND MOTOAKI SATO, *U. S. Geological Survey, Washington, D. C. 20242.*

ABSTRACT

The temperature—oxygen fugacity relationships of the “oxygen buffer” assemblages Ni-NiO, Mn₃O₄-Mn₂O₃, and Mn_{1-x}O-Mn₃O₄ have been determined at 1 atm total pressure by an electrochemical method, over the temperature ranges 519°–1319°, 594°–952°, and 771°–1202°C, respectively.

$$\begin{array}{ll} \text{Ni-NiO} & \log f_{\text{O}_2}(\text{atm}) = 9.36 - \frac{24930}{^\circ\text{K}} \\ \text{Mn}_3\text{O}_4\text{-Mn}_2\text{O}_3 & \log f_{\text{O}_2}(\text{atm}) = 7.34 - \frac{9265}{^\circ\text{K}} \\ \text{Mn}_{1-x}\text{O-Mn}_3\text{O}_4 & \log f_{\text{O}_2}(\text{atm}) = 13.38 - \frac{25680}{^\circ\text{K}} \end{array}$$

These equations will be useful for hydrothermal experimentation and metamorphic petrogenesis, where a knowledge of existing oxygen fugacities is necessary.

INTRODUCTION

The temperature-oxygen fugacity relationships of the manganese oxides are important in the interpretation of the history of metamorphosed manganese oxide deposits. Furthermore, the use of manganese oxide assemblages to buffer the oxygen fugacity in experimental systems (Huebner, 1969) has necessitated the accurate determination of the oxygen fugacities of these assemblages. The present work presents data for the manganosite-hausmannite (Mn_{1-x}O-Mn₃O₄) and hausmannite-bixbyite (Mn₃O₄-Mn₂O₃) buffers at 1 atm total pressure. Data are also included for the nickel-nickel oxide (Ni-NiO) assemblage, a commonly used oxygen buffer in experimental investigations. The uncertainties in the data have been critically examined to show the reliability of the data.

EXPERIMENTAL METHOD

A high-temperature electrochemical method, modified after that of Kiukkola and Wagner (1957) was used to determine the oxygen fugacity ratio between a sample assemblage and a reference oxygen source. A dense, flat-bottomed tube of zirconia-calcia solid solution of the composition, 85 mole percent ZrO₂—15 mole percent CaO, was used to physically separate the sample from a stream of gas of known oxygen fugacity. The zirconia ceramic has a high mobility of oxygen ions at elevated temperatures because of oxygen vacancies in its fluorite-type structure, and hence functions as an anionic solid electrolyte (Kingery *et al.*, 1959). The experiments consist of measuring the EMF of the cell

Reference gas (air), Pt | (Zr,Ca)O₂ | Pt, sample

¹ Publication authorized by the Director, U. S. Geological Survey.

which obeys the Nernst relationship

$$EMF = \frac{RT}{4F} \ln \frac{f_{O_2}(\text{sample})}{f_{O_2}(\text{reference})} \quad (1)$$

A finely ground mixture of the two solids ($Mn_{1-x}O$ and Mn_3O_4 ; Mn_3O_4 and Mn_2O_3 ; or Ni and NiO) was placed in a cup of platinum (or silver-palladium alloy) foil and attached to an electrical lead of the same metal (Fig. 1). The cup with about 300 mg of sample was pressed into the closed end of a stabilized zirconia tube which is about 15 cm long. An alumina tube filled the void, and the tube assembly was sealed with a teflon high-vacuum connector. The sample cup served as the inner electrode and a platinum mesh was the outer electrode of the cell. This method differs from that of previous investigators except Schmalzried (1962) in that the sample and the reference atmospheres are separated by a continuous wall of zirconia, minimizing gas diffusion. (Charette and Flengas (1968) concurrently used a similar cell geometry, isolating the sample and reference chambers.) The cell, or oxygen probe, was placed in a cylindrical furnace through which a reference gas, usually air, was slowly passed at 1 atmosphere pressure. Temperature was measured with a Pt-Pt₉₀Rh₁₀ thermocouple adjacent to the probe. A temperature controller was programmed in ascending and descending increments and temperature was continuously monitored on one channel of a two-pen recorder. This recorder channel was calibrated with both a known voltage source and the thermocouple EMF at the melting point of gold, 1063°C. (Appendix I contains all the equations based on the IPTS 1968, with melting point of gold at 1064.4°C.) Temperature was maintained constant for at least 1–3 hours between changes. An electrometer with a high input impedance (10^4 ohms) was used as an impedance matching device between the electrochemical cell and the second channel of the recorder. The electrometer-recorder combination was calibrated against a known voltage source.

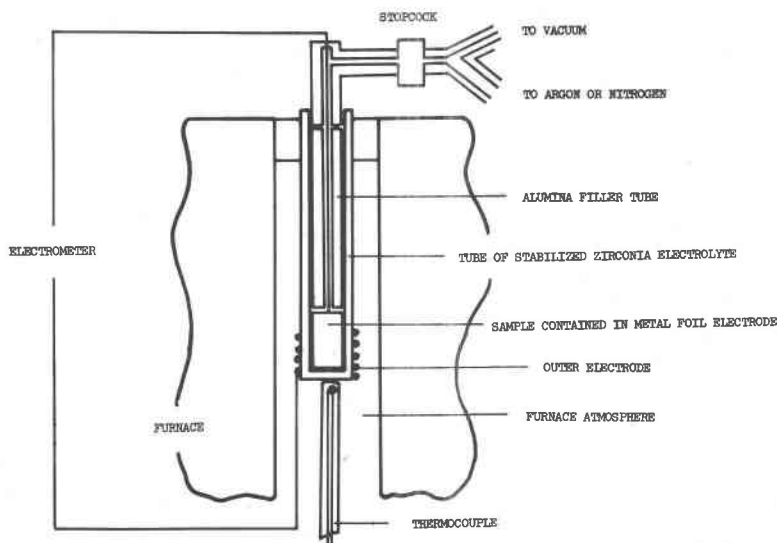


FIG. 1. Schematic diagram of experimental apparatus with a single oxygen probe in position.

For experiments in which silver-palladium alloy (40 wt. % Pd) was used within the probe, the measured EMF was corrected for the voltage induced by the metal junction, outer Pt, Ag₆₀Pd₄₀ inner foil, to yield the cell EMF. The correction varied from 10 to 35 mv, depending upon the temperature,¹ and was subtracted from the measured EMF.

The rate of oxygen diffusion through the stabilized zirconia ceramic is small, but finite (Ullmann, 1968). To reduce diffusion in several of the experiments, the magnitude of the oxygen fugacity of the furnace atmosphere (a mixture of N₂ or Ar, H₂O, and H₂) was maintained at approximately the value of the sample oxygen fugacity by an electrolytic method described by Sato (1970). In this case, a second oxygen probe was placed in the furnace to measure the f_{O_2} of the furnace atmosphere. Air circulated through the interior of the second probe and provided a reference f_{O_2} . The EMF of the sample probe is a measure of the difference between the oxygen fugacity of the sample and of the furnace atmosphere. The output of this cell can be used to regulate the f_{O_2} of the furnace atmosphere. When the EMF = 0 volts, f_{O_2} values of furnace atmosphere and of the sample are identical if platinum foil and lead wire are used for measuring the sample. The second probe then measures the sample f_{O_2} . Conversely, when both reference and furnace atmospheres are air, this additional oxygen probe reads 0 volts (experimentally, <0.001 volt).

DATA REDUCTION

Recorder traces were converted to tabulations (Appendix II²) of temperature versus oxygen fugacity and then subjected to a least-squares refinement. Data were forced to fit a first degree equation on the assumption that the ΔH° of reaction is independent of temperature. This assumption is probably valid when the stoichiometry of the solid phases does not change, but may not hold rigorously when manganosite (Mn_{1-x}O) participates in a reaction. Equations for the reactions are presented as a function of temperature (°K) and log oxygen fugacity (atm). Equations based on the International Practical Temperature Scale of 1948 are given in the text for purposes of comparison with previous data. Appendix I contains equations based on the new temperature scale, IPTS 1968 (Benedict, 1969; Comité International des Poids et Mesures, 1969). Uncertainties reported are one standard error of the mean, assuming all the variation to be in the oxygen fugacity. Standard deviations σ are given for each equation to indicate the scatter of individual measurements about the regression line.

SYSTEMATIC ERRORS

Systematic errors are caused by errors in calibration and bias in measurement. The uncertainties in the results contributed by systematic errors are small. Thermocouple EMF could be read to the nearest 0.01 millivolt. Estimated uncertainty due to thermocouple calibration and to real differences in temperature between the thermocouple and sample probe position are estimated at 0.02 mv (2°C). Overall temperature uncertainty is probably within $\pm 3^\circ\text{C}$. Cell EMF could be read to about ± 1 millivolt; drift was within ± 2 millivolts per run; calibration within ± 1 millivolt. At 900°C the uncertainty in temperature measurement causes an uncertainty of ± 0.02 log units of oxygen fugacity,

¹ EMF correction (millivolts) = $-2.4368 + 2.2293X + 0.04633X^2$ where X is the output (in millivolts) of a Pt-Pt₉₀Rh₁₀ thermocouple at the same temperature as the Pt-Ag₆₀Pd₄₀ junction.

² To obtain a copy of experimental results in tabular form, order NAPS Document No. 00944 from National Auxiliary Publications Service of the A.S.I.S., c/o CCM Information Corporation, 909 Third Avenue, New York, New York 10022, remitting \$2.00 for microfiche or \$5.00 for photocopies, in advance payable to CCMIC-NAPS.

and the uncertainty in measuring the cell EMF causes an uncertainty of 0.07 log units in the oxygen fugacity. The total systematic error is within ± 0.1 to ± 0.15 log unit of oxygen fugacity, depending upon temperature.

PREPARATION OF STARTING MATERIALS

The hausmannite and bixbyite used in this study are the same materials prepared and used by Huebner (1969). Fresh manganosite was prepared by reducing pyrolusite (MnO_2) in a stream of hydrogen at 800°C . Nickel and nickel oxide were supplied by Fisher Scientific Company (Lots no. 783281 and no. 784016, respectively).

NI-NiO BUFFER

To validate the experimental results of this study, the f_{O_2} - T relationship of the nickel-nickel oxide assemblage was measured. The results were compared with those obtained by previous investigators who used several different methods. The agreement is good, hence the f_{O_2} - T relationship presented here is apparently at least as reliable as that reported by other investigators.

The Ni-NiO buffer was run four times, resulting in 118 measurements of oxygen fugacity over the temperature range 519° – 1319°C . Runs NNO (1) and (4) were made in a furnace atmosphere of air (Figure 2); least-squares refinement of the resultant 57 measurements yielded the equation

$$\log f_{\text{O}_2}(\pm 0.03) = 9.45 - \frac{24930}{T} ; \quad \sigma = 0.22 \quad (2)$$

At higher temperature, there is increased diffusion of molecular oxygen through the stabilized zirconia ceramic in response to an oxygen fugacity gradient: f_{O_2} in the furnace atmosphere (air) is 0.210 atm, whereas the f_{O_2} in the probe varies from approximately 10^{-6} to 10^{-22} atm. If the solid phases could not react quickly enough to prevent the f_{O_2} of the atmosphere within the sample chamber from rising above the equilibrium f_{O_2} of the solid buffer, the measured f_{O_2} values would be anomalously high. This possibility was minimized in runs NNO (2) and (3). In this case the furnace atmosphere consisted dominantly of nitrogen or argon saturated with water vapor at room temperature. Electrolytic hydrogen was added to the gas flowing into the furnace such that the f_{O_2} , which is controlled by the $\text{H}_2\text{O}/\text{H}_2$ ratio, was close to that of the sample. The sample and furnace atmosphere compositions are grossly similar (mostly an inert gas such as nitrogen or argon). The oxygen fugacities are nearly the same (sample probe EMF commonly ± 0.05 to 0.10 volt), and both have small amounts of H_2O , in the case of the sample due to absorbed water, and in the furnace supplied by the stream of nitrogen saturated with water vapor at room temperature (Sato, 1970). It is reasonable to expect that the hydrogen fugacities of the sample and furnace atmospheres would

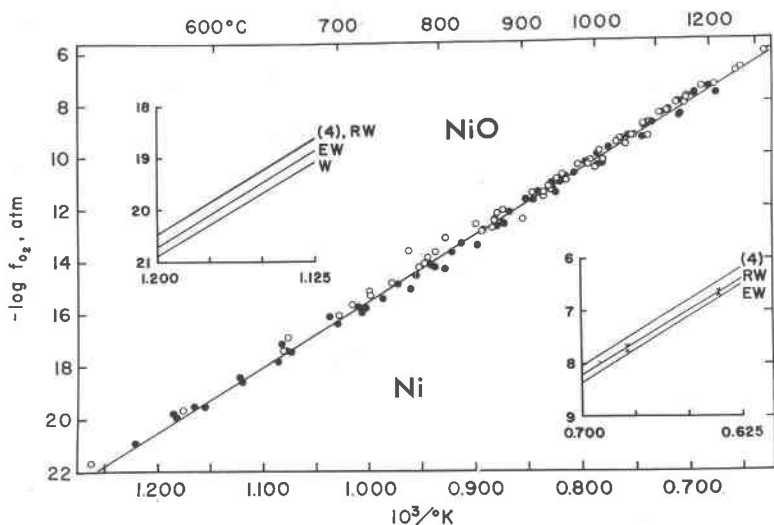


FIG. 2. Position of the Ni-NiO equilibrium, equation (4). Open circles represent measurements for which the furnace atmosphere was air. Solid dots represent measurements in a reducing furnace atmosphere. Insets compare $\log f_{O_2}$ versus $1/T^\circ K$ values calculated from equation (4) with $\log f_{O_2}$ versus $1/T^\circ K$ values given by other investigators: EW is Eugster and Wones (1962); W is Watanabe (1933); RW is Robie and Waldbaum (1968); ∇ and \wedge are bracketing runs by Hahn and Muan (1961).

be similar. In any event the H_2O/H_2 mixing ratio is on the order of 100 and the initial f_{H_2O} is about 0.03 atm. Assuming f_{H_2} in the furnace to be 0.0003 atm, this low hydrogen fugacity probably would not cause transport of appreciable quantities of hydrogen into (or out of) the sample chamber. Runs NNO (2) and (3) (Figure 2) yielded 61 measurements described by the equation

$$\log f_{O_2}(\pm 0.03) = 9.21 - \frac{24760}{T}; \quad \sigma = 0.25 \quad (3)$$

The oxygen fugacity values given by equation (3) are slightly below those of equation (2) and suggest that oxygen diffusion is minimized; however, the difference is probably not significant.

Over the temperature range of interest, 400°–1000°C, there is not a great difference between these equations: within 0.01 $\log f_{O_2}$ unit at 400°C, and 0.11 $\log f_{O_2}$ unit at 1000°C. These differences are of the same order of magnitude as the systematic errors of the experiments, and one-half to one-third the magnitude of the standard deviation (random error). The preferred f_{O_2} - T relation for the Ni-NiO assemblage at one atmosphere pressure is the regression of all 118 data points:

$$\log f_{\text{O}_2}(\pm 0.02) = 9.31 - \frac{24810}{T}; \quad \sigma = 0.24 \quad (4)$$

The standard error of the estimate of the dependent variable is $\sigma = 0.24$ log f_{O_2} units, whereas the standard error of the mean is 0.02 units. This latter value, a measure of statistical error in the placement of the Ni-NiO reaction curve at the 68% confidence level, is much smaller than the estimated limits of the systematic error, discussed earlier.

Oxygen fugacity-temperature relations determined in this and certain previous investigations are plotted in Figure 2. Agreement between various methods is good. Kiukkola and Wagner (1957) sandwiched a wafer of electrolyte (85% ZrO_2 —15% CaO) between nickel-nickel oxide and iron-wüstite assemblages and measured the EMF of the resultant cell. Despite the fact that oxygen could have diffused between the Ni-NiO and the reference $\text{Fe-Fe}_{1-x}\text{O}$, their results agree well with ours. Charette and Flengas (1968) used a closed stabilized zirconia tube to separate the Ni+NiO mix from the oxygen reference. Watanabe (1933), Antill and Warburton (1967) and Fricke and Weitbrecht (1942) measured the CO_2/CO ratios in equilibrium with the Ni-NiO assemblage. The data of Watanabe and of Fricke and Weitbrecht result in lower f_{O_2} values. Note that the measured CO_2/CO ratios of the last-named investigators were used to calculate log f_{O_2} values. Hahn and Muan (1961) determined the conditions of reaction between nickel and nickel oxide in CO_2/H_2 gas mixtures whose f_{O_2} could be calculated from the mixing ratios; their four values plot 0.3 log units below the present results. Eugster and Wones (1962) summarized thermochemical values and presented an equation which gives f_{O_2} values that are too low.

The enthalpy of the reaction $\text{Ni} + 1/2\text{O}_2 = \text{NiO}$ calculated from equation (4), is -56.76 ± 0.30 kcal/mole NiO.¹ Coughlin (1954) gives -56.74 ± 0.1 kcal at 1200°K, the midpoint of the temperature measurement range in this investigation, based on data that include reaction equilibrium measurements. Boyle *et al.* (1954) give the value $\Delta H^\circ_{298.16} = -57.3 \pm 1$ kcal/mole, based solely upon combustion calorimetry. The value presented by Robie and Waldbaum (1968), based solely upon calorimetric measurements, is more positive: -55.993 ± 0.100 kcal at 1200°K; ranging from -56.519 kcal at 700°K to -55.697 at 1500°K.

The standard free energy of formation of 2 NiO is calculated by substituting the expression $\Delta G^\circ = -RT \ln K$ into equation (4), yielding (cal)²

$$\Delta G^\circ_{\text{T}}(\pm 124) = 42.62T - 113500 \quad (5)$$

¹ Based on equation (3), $\Delta H^\circ_{\text{R}} = 56.65 \pm 0.03$ kcal.

² Based on equation (3), $\Delta G^\circ_{\text{R}} = 42.12 T - 113300$, in calories.

Free-energy values calculated from equation (5) are compared in Table 1 with the tabulated values given by Robie and Waldbaum (1968), whose values are based on calorimetric data, and by Coughlin (1954), whose values are based on reduction equilibria measurements. Agreement is good at 700°K, but significant differences are present at higher temperatures. Agreement is also good with an equation given by Rizzo *et al.* (1967); an electrochemical cell was used, but the data are not given.

TABLE 1. STANDARD FREE ENERGY OF FORMATION ΔG_f° , 2 MOLES OF NiO AT 1 ATM

$T_{48}, ^\circ\text{K}$	Equation (5)	Robie and Waldbaum (1968)	Coughlin (1954)	Equation 5' (IPTS 1968)
298.16		-101.148(± 0.220)	-101.24(± 0.280)	
700	-83.69	-83.758	-83.38	-84.10
800	-79.43	-79.594	-78.96	-79.82
900	-75.17	-75.464	-74.54	-75.54
1000	-70.90	-71.334	-70.16	-71.26
1100	-66.64	-67.270	-65.80	-66.98
1200	-62.38	-63.168	-61.44	-62.70
1300	-58.12	-59.126	-57.12	-58.42
1400	-53.86	-55.072	-52.82	-54.13
1500	-49.60	-51.022	-48.52	-49.85
1600	-45.33	-47.002	-44.26	-45.57

$\text{Mn}_3\text{O}_4\text{-Mn}_2\text{O}_3$ BUFFER

The oxygen fugacity-temperature relationship of the assemblage $\text{Mn}_3\text{O}_4\text{-Mn}_2\text{O}_3$ has been investigated by many workers using a variety of methods, but the agreement between individual investigators and the different methods is not good. Neither do these data seem to be of sufficiently good quality to be extrapolated to lower temperatures. The methods and results of previous investigations are summarized in Table 2.

A finely ground mixture of approximately equal parts of Mn_3O_4 and Mn_2O_3 was contained in a platinum foil cup. The oxygen probe was placed in a stream of air within the furnace. The oxygen chemical potential gradient across the stabilized zirconia ceramic is relatively small. In view of the results of the Ni-NiO experiments and the relatively high f_{O_2} values of the $\text{Mn}_3\text{O}_4\text{-Mn}_2\text{O}_3$ buffer, it is not expected that oxygen diffusion would noticeably effect the results of the experiment.

Forty-three measurements over the temperature range 594–952°C (Figure 3) resulted in the equation

$$\log f_{\text{O}_2}(\pm 0.02) = 7.36 - \frac{9280}{T}; \quad \sigma = 0.12 \quad (6)$$

TABLE 2. SUMMARY OF INVESTIGATIONS OF THE REACTION $4 \text{Mn}_3\text{O}_4 + \text{O}_2 = 6 \text{Mn}_2\text{O}_3$

	Temperature Range, °K	Equation of Reaction (in atm)	Number of Mea- sure- ments
Electrochemical measurement of f_{O_2}			
Present investigation	867-1225	$\log f_{\text{O}_2} = 7.36 - \frac{9280}{T}$	43
Charette and Flengas (1968)	875-1125	$\log f_{\text{O}_2} = 9.56 - \frac{11850}{T}$	6
Detection of phase change at controlled f_{O_2} and T			
Hahn and Muan (1960)	1143-1245	$\log f_{\text{O}_2} = 8.05 - \frac{10100}{T}$	3
Matsushima and Thoburn (1965)	797-851	$\log P_{\text{O}_2} = 4.00 - \frac{5000}{T}$	12
Klingsberg and Roy (1960)	1158	$\log f_{\text{O}_2} = -0.68 \text{ at } 1158^\circ\text{K}$	1
Measurement of P_{O_2} by manometer			
Ingraham (1966)	1066-1193	$\log P_{\text{O}_2} = 8.98 - \frac{10965}{T}$	21
Otto (1964)	1132-1247	$\log P_{\text{O}_2} = 7.19 - \frac{9004}{T}$	21
Shenouda and Aziz (1967)	868-942	$\log P_{\text{O}_2} = 8.268 - \frac{10240}{T}$	9
Schmahl and Stemmler (1965)	?	$\log P_{\text{O}_2} = 7.8205 - \frac{9909.7}{T}$?
Vlasov and Kozlov (1958)	1023-1123	$\log P_{\text{O}_2} = 8.57 - \frac{11040}{T}$	3
Measurement of P_{O_2} by thermal conductivity gas analysis			
Hochgeschwender and Ingraham (1967)	968-1043	$\log P_{\text{O}_2} = 8.982 - \frac{11216}{T}$	21
Measurement of P_{O_2} by filament resistance measurement			
Kim <i>et al.</i> (1966)	823-1293	$\log P_{\text{O}_2} = 6.97 - \frac{9420}{T}$	7
From thermochemical (heat content) measurements			
Mah (1960)		$\log f_{\text{O}_2} = 7.08 - \frac{9790}{T}$	
Robie and Waldbaum (1968)		$\log f_{\text{O}_2} = 7.62 - \frac{9497}{T}$	

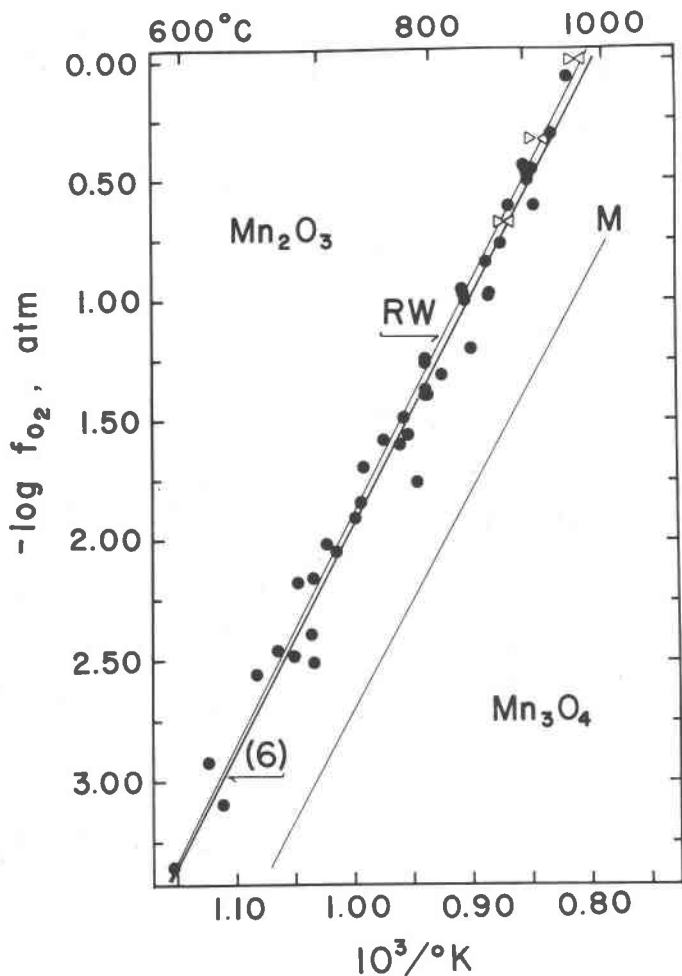


FIG. 3. Data for the equilibrium Mn_3O_4 - Mn_2O_3 -Gas. Circles represent measurements used in calculating equation (6), the heavy line. Triangles represent bracketing runs by Hahn and Muan (1960). Thin lines are calculated from tabulated free energies of formation, M for Mah (1960) and RW for Robie and Waldbaum (1968).

The relatively great temperature range of the experiments and the small standard error of the mean, 0.02 log atm units, suggest that this equation may be extrapolated to the lower temperatures ($> 300^\circ\text{C}$) that were used by Huebner (1969) and that are characteristic of environments of low to intermediate metamorphic grade.

A plot (Figure 3) of equation (6) passes very near (within experimental

error) the three bracketing values given by Hahn and Muan (1960). The results reported in the present paper were determined over a much greater range of temperature to define more accurately the slope of the reaction $\text{Mn}_3\text{O}_4\text{-Mn}_2\text{O}_3\text{-Gas}$. With decreasing temperature equation (6) diverges toward higher f_{O_2} with respect to the equation given by Hahn and Muan. Two other investigators, Otto (1964) and Shenouda and Aziz (1967), present equations similar to equation (6), but the experimental ranges of temperature are limited (see Table 2) and do not permit extrapolation. However, it is interesting to note that over the temperature range 850° to 950°C , the equations of several investigators give $\log f_{\text{O}_2}$ values within $\pm 0.2 \log f_{\text{O}_2}$ units of equation (6). Charette and Flengas (1968), whose results for Ni-NiO agree well with ours, disagree in their results for $\text{Mn}_3\text{O}_4\text{-Mn}_2\text{O}_3$, using Ni-NiO as a reference assemblage. They reported unstable EMF values for the $\text{Mn}_3\text{O}_4\text{-Mn}_2\text{O}_3$ assemblage, in contrast to our stable values.

The enthalpy of the reaction $4 \text{Mn}_3\text{O}_4 + \text{O}_2 = 6 \text{Mn}_2\text{O}_3$ calculated from equation (6) is 42.46 ± 0.09 kcal, compared with the 46.2 ± 3.3 kcal given by Hahn and Muan, 43.65 and 41.1 given by Mah (1960) for 900°K and 1100°K , respectively, and 45.060 and 42.506 kcal given by Robie and Waldbaum (1968) for 900° and 1100°K . The Gibbs free energy of reaction derived from equation (6) does not agree well with the thermochemical data (Mah, 1960) as can be deduced from Figure 3. The explanation for this discrepancy may be poor entropy data at temperatures approaching absolute zero (Robie, oral communication). Robie and Waldbaum (1968) combined the best heat-content data (summarized by Mah (1960)) with new values of S°_{298} for Mn_3O_4 and enthalpy of formation for Mn_2O_3 calculated by Otto (1964) from vapor pressure measurements to obtain free energies of formation for Mn_3O_4 and Mn_2O_3 . Agreement with the data presented here is excellent (see Fig. 3). Although Otto's vapor-pressure curve for the $\text{Mn}_3\text{O}_4\text{-Mn}_2\text{O}_3$ reaction has a different slope and intercept (Table 2), agreement with Robie and Waldbaum (1968) is so good that we have chosen not to present new values for the entropy and enthalpy of formation of Mn_2O_3 or Mn_3O_4 .

$\text{Mn}_{1-x}\text{O-Mn}_3\text{O}_4$ BUFFER

The manganosite-hausmannite buffer, $\text{Mn}_{1-x}\text{O-Mn}_3\text{O}_4$, has been used to control the oxygen fugacity of a $\text{CO}_2\text{-CO}$ gas (Huebner, 1969) and of a $\text{H}_2\text{O-H}_2$ fluid (Huebner, 1967; Ernst, 1966; Gilbert, 1966; and Lindsley, 1963). One of us (JSH) has determined the relative oxygen fugacity values of the manganosite-hausmannite, magnetite-hematite, and nickel-nickel oxide buffers by using the hydrothermal buffer technique (Eugster, 1957; Eugster and Wones, 1962). Runs tabulated in

TABLE 3. BUFFERED HYDROTHERMAL EXPERIMENTS INDICATING RELATIVE POSITION OF MANGANOSITE-HAUSMANNITE BUFFER

P _T =2000 bars				
T°C.	Time, days	Buffer	Charge Reactants	Charge Products
753 ± 4	7	Fe ₃ O ₄ -Fe ₂ O ₃	MnO, H ₂ O	Mn ₃ O ₄ , H ₂ O (trace MnO)
695 ± 6	11	Fe ₃ O ₄ -Fe ₂ O ₃	MnO, H ₂ O	Mn ₃ O ₄ , MnO, H ₂ O
685 ± 14	13	Fe ₃ O ₄ -Fe ₂ O ₃	MnO, H ₂ O	Mn ₃ O ₄ , MnO, H ₂ O
656 ± 9	111	Fe ₃ O ₄ -Fe ₂ O ₃	MnO, H ₂ O	Mn ₃ O ₄ , MnO, H ₂ O
650 ± 14	6	Fe ₃ O ₄ -Fe ₂ O ₃	MnO, Mn ₃ O ₄ , H ₂ O	MnO, Mn ₃ O ₄ , H ₂ O
622 ± 13	36	Fe ₃ O ₄ -Fe ₂ O ₃	MnO, H ₂ O	MnO, Mn(OH) ₂ , H ₂ O ^a
605 ± 9	126	Fe ₃ O ₄ -Fe ₂ O ₃	MnO, H ₂ O	Mn ₃ O ₄ , MnO, H ₂ O
558 ± 7	32	Fe ₃ O ₄ -Fe ₂ O ₃	Mn ₃ O ₄ , H ₂ O	Mn ₃ O ₄ , H ₂ O
709 ± 8	7	Ni-NiO	Mn ₃ O ₄ , H ₂ O	MnO, H ₂ O
558 ± 11	25	Ni-NiO	Mn ₃ O ₄ , H ₂ O	MnO, H ₂ O

^a Mn(OH)₂ is a quench product.

Table 3 indicate that the manganosite-hausmannite assemblage is more reducing than the magnetite-hematite assemblage at 2000 atm over the temperature range 605°–753°C and less reducing than the Ni-NiO assemblage at 558° and 709°C.

Manganosite, Mn_{1-x}O, is similar to wüstite in that it is non-stoichiometric due to cation deficiency. Davies and Richardson (1958) report that between 1500° and 1650°C, the manganosite composition is independent of temperature but varies from Mn_{1.000}O to Mn_{0.957}O as a function of oxygen fugacity. Schwerdtfeger and Muan (1967) show similar results at 1200° and 1400°C. Voeltzel and Manenc (1967) suggest that manganosite is nearly stoichiometric at 1100°C. Hed and Tannhauser (1967) investigated the system Mn-O and report that near the manganosite-hausmannite boundary, manganosite is appreciably cation deficient (to Mn_{0.87}O); extrapolation of their data suggests that compositions as oxygen rich as Mn_{0.95-0.97}O are not unreasonable at the conditions of this study. Muan and Hahn (1959) discuss the effect of variable manganosite composition on phase diagrams. Obviously the activity of MnO is not unity under these conditions, and thermochemical calculations based upon stoichiometric MnO are not sufficient for practical applications.

Hausmannite, Mn₃O₄, has been shown to be stoichiometric at a variety of conditions by Hahn and Muan (1960), Hed and Tannhauser (1967), Shomate (1943), and Moore *et al.* (1950). The results of LeBlanc and Wehner (1934) which indicate deviation from the ideal formula MnO_{1.333}, are suspect because their samples may not have been homogeneous. Only

Driessens (1967) suggests that the hausmannite composition is variable (see next paragraph), but in the absence of analytical data, it is probably safe to assume that $a_{\text{Mn}_3\text{O}_4} = 1.00$ for the purposes of this study.

Hausmannite can be visualized as a tetragonally distorted spinel at room temperatures (Aminoff, 1926) and a cubic spinel at high temperatures (McMurdie and Golovato, 1948). The transition temperature has been placed at 1170°C (McMurdie *et al.*, 1950), $1172 \pm 40^\circ$ (Southard and Moore, 1942) $1160 \pm 5^\circ$ (Van Hook and Keith, 1958), $1132^\circ \pm 18^\circ$ in air (Driessens, 1967) and below $1120^\circ \pm 10^\circ$ in carbon dioxide (Driessens, 1967). The tetragonal to cubic inversion is accompanied by a significant change in heat content (Mah, 1960; Robie and Waldbaum, 1968); a curve relating $\log f_{\text{O}_2}$ and $1/T$ is expected to undergo a considerable change of slope at the transition temperature (see Fig. 4). It is not valid, therefore, to extrapolate f_{O_2} - T data for the manganosite-cubic Mn_3O_4 -Gas reaction (as done by Ernst, 1966; Gilbert, 1966; and Lindsley, 1963) without first evaluating the effects of this transition.

Previous investigations of the Mn_{1-x}O - Mn_3O_4 -Gas equilibrium are tabulated in Table 4. None of these investigations agrees with available calorimetric data (Figure 4), and none shows the change of slope expected from the measured heat contents. There is disagreement between different investigators. Only Blumenthal and Whitmore (1961) and Schwerdtfeger and Muan (1967, published after the present investigation of this reaction was nearly completed) give sufficient data to determine accurately the reaction below the transition of Mn_3O_4 . Blumenthal and Whitmore's data lie at higher f_{O_2} values than an extrapolation of the Hahn and Muan (1960) curve, although the thermochemical data suggests lower f_{O_2} values below the transition. Furthermore, Blumenthal and Whitmore's data for the magnetite-hematite assemblage, similarly obtained, are suspect (Haas, personal communication). The thermochemical data for the manganosite-hausmannite buffer (Mah, 1960) indicate f_{O_2} values above the magnetite-hematite buffer at temperatures greater than 700°C, in contradiction of the results of Table 3. For these reasons it was considered worthwhile to undertake a reinvestigation of the manganosite-hausmannite (tetragonal) equilibrium, taking care to approach equilibrium as closely as possible.

The initial electrochemical measurements of f_{O_2} of the manganosite-hausmannite buffer indicated generally consistent results for a single run, but disagreement between runs. Most runs fell within a range of one log unit f_{O_2} at any given temperature. Several runs gave smooth curves whose slope decreased with temperature (Fig. 4); one such smooth curve plotted 2 to 3 log units above the nearest data. Other runs plotted as straight lines in $1/T^\circ\text{K}$ - $\log f_{\text{O}_2}$ space. One possible explanation is that one solid

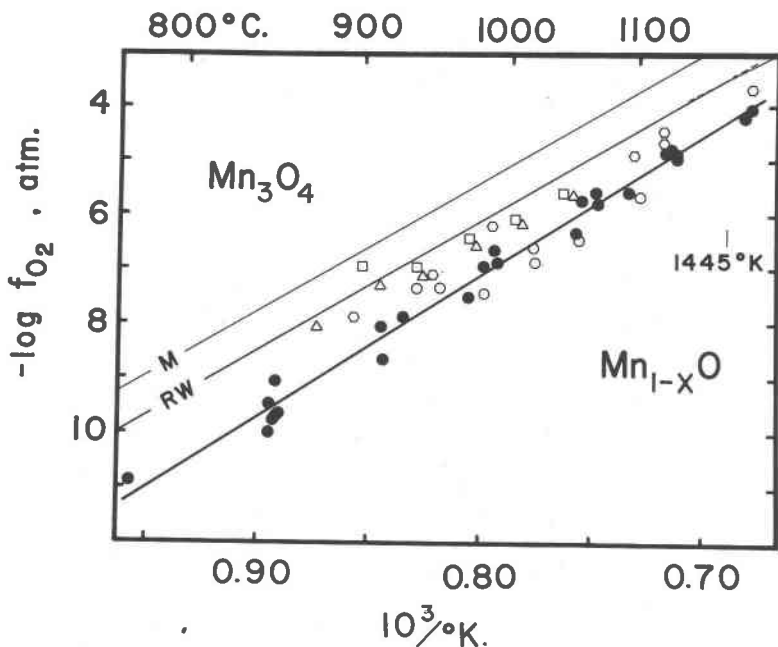


FIG. 4. Data for the equilibrium manganosite-hausmannite-gas, used to calculate equation (7). Solid dots represent measurements in fused KCl-NaCl used to obtain equation (7), shown as a heavy line. Tabulated free energy values yield the thin lines M (Mah, 1960) and RW (Robie and Waldbaum, 1968). The tetragonal-cubic transition of Mn_3O_4 is placed at 1445°K . Squares, triangles, hexagons, and open circles are measurements of four different runs in which halide melt was not present.

phase with a broad compositional range, in this case manganosite, controls the oxygen fugacity, disregarding the presence of the other solid phase. Only one manganosite-hausmannite curve can be truly stable; all other possible curves are metastable. We suspect that our anomalous initial results are due to the persistence of manganosite of metastable composition and failure of attainment of true equilibrium. Unfortunately, there is no simple way to determine the manganosite composition in the oxygen probe without quenching.

In order to accelerate the attainment of stable equilibrium, a chloride melt was added to the sample. A KCl-NaCl melt added to the sample produced consistent and reproducible results with both increasing and decreasing temperatures. Evidently the presence of the flux accelerated the change of composition of manganosite to the one which is in true equilibrium with hausmannite. Comparison of cell dimensions of manganosite and hausmannite made before and after the runs did not show

TABLE 4. SUMMARY OF INVESTIGATIONS OF THE REACTION $6 \text{ "MnO"} + \text{O}_2 = 2 \text{ Mn}_3\text{O}_4$

Reference	Method	Temp. Range °K	Observations	$\log f_{\text{O}_2}$, atm
Present investigation	A	1044-1475	25	$13.42 - \frac{25710}{T}$
Schwerdtfeger and Muan (1967)	A	1198-1473	11	$11.54 - \frac{23295}{T}$
Blumenthal and Whitmore (1961)	A	1078-1323	34	$11.71 - \frac{23468}{T}$
Charette and Flengas (1968)	A	992-1393	13	$11.56 - \frac{23234}{T}$
Hahn and Muan (1960)	B	1540-1785	5	$13.31 - \frac{26000}{T}$
Kim <i>et al.</i> (1966)	C	813-1423	7	$15.70 - \frac{25100}{T}$
Isihara and Kigoshi (1953)	B	773-1073	4	$9.76 - \frac{28800}{T}$

A. Electrochemical method using stabilized zirconia electrolyte.

B. Gas mixing furnace.

C. Oxygen pressure measurement by filament resistance.

significant differences. Although cell dimensions do not indicate the oxygen content, they should reflect the entry of the large Na^+ , K^+ , or Cl^- ions into the oxide structure.

Twenty-five measurements (Figure 4) of T and f_{O_2} determined in the presence of a KCl-NaCl melt were refined, yielding the equation

$$\log f_{\text{O}_2}(\pm 0.05) = 13.42 - \frac{25710}{T}; \quad \sigma = 0.24 \quad (7)$$

There is no appreciable difference between $\log f_{\text{O}_2}$ values measured on increasing and decreasing temperature profiles. The standard deviation is 0.24; the standard error of the mean (statistical uncertainty in placement of the curve) is $\pm 0.05 \log f_{\text{O}_2}$ units. Two of the measured f_{O_2} values were made above but close to the cubic-tetragonal Mn_3O_4 transition temperature; since the deviation in f_{O_2} due to the transition is not significant at the temperature of these two measurements, they were included in the refinement.

Equation (7) is compared with the results of previous investigators in Table 4. Our data below the transition result in a slope nearly identical

to that found by Hahn and Muan (1960) above the transition and lie about 0.3 log f_{O_2} units above the earlier results. Evidently the Mn_3O_4 transition does not significantly affect the slope of the reaction. Electrochemical measurements by Schwerdtfeger and Muan (1967) agree very well with our measurements below 1000°C, and fall at slightly lower f_{O_2} values above 1000°C. Their data tend toward an extrapolation of the Hahn and Muan curve. Charette and Flengas (1968) and Blumenthal and Whitmore (1961) obtained higher f_{O_2} values than the present investigators.

Equation (7) was obtained by forcing a linear equation to fit the data points; that is, assuming both $a_{Mn_{1-x}O}$ and ΔH°_R to be constant. Visual inspection of Figure 4 suggests that the fitting of a higher order curve to the data is not warranted. Within the limits of the data, it is probably safe to state that the manganosite activity is constant over the temperature range considered, 771°–1202°C.

The ΔH°_R of the manganosite-hausmannite buffer reaction is 117.7 \pm 1.6 kcal, which compares with 118.5 \pm 2.5 reported by Hahn and Muan (1960) and 109.4–106.7 over the temperature range of interest (Mah, 1960; Robie and Waldbaum, 1968). The free energy of reaction is given by the equation (in cal)

$$\Delta G_R^\circ = 61.41 T - 117600 \quad (8)$$

but the stoichiometry of the reaction is not defined. The thermochemical data (Mah, 1960) yield higher f_{O_2} values (Fig. 4) because the free energy of reaction is smaller. Adjusted values of Robie and Waldbaum (1968) for Mn_3O_4 yield better agreement with equation (7), and fall close to some electrochemical measurements (Fig. 4) which gave anomalously high f_{O_2} values. The manganosite used for the heat content measurements was prepared by reducing higher oxides in hydrogen (Southard and Shomate, 1942). Assuming the thermochemical data for Mn_3O_4 to be correct, a not unreasonable assumption in view of the excellent agreement between Robie and Waldbaum (1968) and this investigation for the Mn_3O_4 - Mn_2O_3 -Gas equilibrium, the discrepancy for the “MnO”- Mn_3O_4 -Gas equilibrium can be explained by the manganosite composition. Even after reduction in hydrogen, manganosite appears to be nonstoichiometric.

Mn_2O_3 - MnO_2 BUFFER

Pyrolusite, MnO_2 , readily decomposes to form Mn_2O_3 in air or oxygen at about 600°C. Because the oxygen probe does not equilibrate readily below about 600°C, and because it cannot tolerate pressure much above one atmosphere, the assemblage Mn_2O_3 - MnO_2 -Gas was not investigated electrochemically. However, the results of this investigation suggest that the values of $\Delta G^\circ_{Mn_2O_3}$ tabulated by Robie and Waldbaum (1968) are

correct, and if we assume their data for $\Delta G^\circ_{\text{MnO}_2}$ to be correct also, the $\log f_{\text{O}_2}$ - T relation for this assemblage can be calculated as

$$\log f_{\text{O}_2} = 11.15 - \frac{8820}{T} \quad (9)$$

This equation is to be preferred over the equation calculated by Huebner (1969) from the data of Mah (1960), although the difference is not great: equation (9) gives $\log f_{\text{O}_2}$ values 0.2 to 0.25 units above the equation previously used.

APPLICATION OF MANGANESE AND NICKEL OXIDE BUFFERS

The application of the manganese oxide and nickel oxide buffers to experimental systems will most commonly be at pressures in excess of one bar, as outlined by Eugster and Wones (1962), French (1964), Huebner (1969), Huebner and Eugster (1969) and Eugster and Skippen (1967). Equations for these buffers are summarized in Table 5. A term has been included to correct the oxygen fugacity for the effect of total pressure on the solid phases (Eugster and Wones, 1962), and is based on molar volume data determined at room temperature and pressure, assuming stoichiometric composition. Use of this term involves the assumption that the molar volume change of the reaction is independent of P and T , that is, the effects of compressibility and thermal expansion tend to cancel (Thompson, 1955; Eugster and Wones, 1962). Molar volumes of solids are from Robie *et al.* (1966); X-ray powder diffraction measurements on materials used in this study confirm the values for Mn_3O_4 and Mn_2O_3 .

ACKNOWLEDGEMENTS

Miss M. Woodruff, U.S. Geological Survey, offered valuable assistance by helping in the interpretation of the strip charts, the computation, and the punching of computer

TABLE 5. EQUATION FOR BUFFER CURVES (ATM) IPTS 1968

Buffer	$\log f_{\text{O}_2}$
$\text{Mn}_{1-x}\text{O}-\text{Mn}_3\text{O}_4$	$13.38 - \frac{25680}{T} + 0.0807 \left(\frac{P-1}{T} \right)$
$\text{Mn}_3\text{O}_4-\text{Mn}_2\text{O}_3$	$7.34 - \frac{9265}{T} + 0.0051 \left(\frac{P-1}{T} \right)$
$\text{Mn}_2\text{O}_3-\text{MnO}_2$	$11.14 - \frac{8810}{T} + 0.019 \left(\frac{P-1}{T} \right)$
$\text{Ni}-\text{NiO}$	$9.36 - \frac{24930}{T} + 0.046 \left(\frac{P-1}{T} \right)$

cards. We particularly appreciate her patience in typing the manuscript with its tables. R. Robie first called the authors' attention to the new temperature scale IPTS 1968. The curve fitting routine used is BMDO5R, "Polynomial Regression", from the package of Biomedical Computer Programs (W. J. Dixon, ed. (1968) *Univ. Calif. Pub. in Automat. Comput.* 2, Univ. Calif. Press).

BIBLIOGRAPHY

- AMINOFF, G. (1926) Über die kristallstruktur von hausmannite (MnMn_2O_4). *Z. Kristallogr.* **64**, 475-490.
- ANTILL, J. E. AND J. B. WARBURTON (1967) Oxidation of nickel by carbon dioxide. *J. Electrochem. Soc.* **114**, 1215-1221.
- BENEDICT, R. P. (1969) International Practical Temperature Scale of 1968. *Leeds and Northrup Tech. J.* **1969**.
- BLUMENTHAL, R. N. AND D. H. WHITMORE (1961) Electrochemical measurements of elevated temperature thermodynamic properties of certain iron and manganese oxide mixtures. *J. Amer. Ceram. Soc.* **44**, 508-512.
- BOYLE, B. J., E. G. KING, AND K. C. CONWAY (1954) Heats of formation of nickel and cobalt oxides (NiO and CoO) of combustion calorimetry. *J. Amer. Chem. Soc.* **76**, 3835-3837.
- CHARETTE, G. G. AND S. N. FLENGAS (1968) Thermodynamic properties of the oxides of Fe, Ni, Pb, Cu, and Mn by EMF measurements. *J. Electrochem. Soc.* **115**, 796-804.
- COMITÉ INTERNATIONAL DES POIDS ET MESURES (1969) The International practical temperature scale of 1968. *Metrologia* **5**, 35-44.
- COUGHLIN, JAMES P. (1954) Contributions to the data of theoretical metallurgy. XII. Heats and free energies of formation of inorganic oxides. *U.S. Bur. Mines Bull.* **542**, 1-80.
- DAVIES, M. W. AND F. D. RICHARDSON (1959) The non-stoichiometry of manganous oxide. *Trans. Faraday Soc.* **55**, 604-610.
- DRIESSENS, F. C. M. (1967) Place and valence of the cations in Mn_2O_4 and some related manganates. *Inorg. Chim. Acta* **1**, 193-201.
- ERNST, W. G. (1966) Synthesis and stability relations of ferrotremolite. *Amer. J. Sci.* **264**, 37-65.
- EUGSTER, H. P. (1957) Heterogeneous reactions involving oxidation and reduction at high pressures and temperatures. *J. Chem. Phys.* **26**, 1760-1761.
- AND G. B. SKIPPEN (1967) Igneous and metamorphic reactions involving gas equilibria. In P. H. Abelson, ed., *Researches in Geochemistry*, Vol. 2, John W. Wiley and Sons, New York.
- AND DAVID R. WONES (1962) Stability relations of the ferruginous biotite, annite. *J. Petrology*, **3**, 81-124.
- FRENCH, B. M. (1964) *Stability of Siderite and Progressive Metamorphism of Iron Formation*. Ph.D. Diss. The Johns Hopkins University, Baltimore, Maryland.
- FRICKE, R. AND G. WEITBRECHT (1942) Die Gleichgewichte CO_2/CO gegen Ni/NiO , bzw. $\text{Ni}+\gamma\text{-Al}_2\text{O}_3/\text{NiAl}_2\text{O}_4$ und ihre Beeinflussung durch den Physikalischen Zustand der festen Reaktionsteilnehmer. *Z. Elektrochem.* **48**, 87-106.
- GILBERT, M. C. (1966) Synthesis and stability relations of the hornblende ferropargasite. *Amer. J. Sci.* **264**, 698-744.
- HAHN, W. C., JR. AND ARNULF MUAN (1960) Studies in the system Mn-O : The Mn_2O_3 - Mn_3O_4 and Mn_3O_4 - MnO equilibria. *Am. J. Sci.* **258**, 66-78.
- AND ——— (1961) Activity measurements in oxide solid solutions: The systems NiO-MgO and NiO-MnO in the temperature interval 1100-1300°C. *J. Phys. Chem. Solids* **19**, 338-348.

- HED, A. Z. AND D. S. TANNHAUSER (1967) High-temperature electrical properties of manganese monoxide. *J. Chem. Phys.* **47**, 2090-2103.
- HOCHGESCHWENDER, K. AND T. R. INGRAHAM (1967) Use of thermal conductivity gas analysis for thermodynamic measurements on the dissociation of CuO , Mn_2O_3 and MnO_2 . *Can. Met. Quart.* **6**, 71-84.
- HUEBNER, J. S. (1967) *Stability Relations of Minerals in the System Mn-Si-C-O*. Ph.D. thesis, The Johns Hopkins University, Baltimore, Maryland.
- (1969) The stability of rhodochrosite in the system manganese-carbon-oxygen. *Amer. Mineral.* **54**, 457-481.
- and H. P. EUGSTER (1969) Rhodochrosite decarbonation in the system $\text{MnO-SiO}_2\text{-CO}_2$ [abstr.]. *Geol. Soc. Amer. Spec. Pap.* **121**, 144-145.
- INGRAHAM, T. R. (1966) Thermodynamics of the Mn-S-O system between 1000°K and 1250°K. *Can. Met. Quart.* **5**, 109-122.
- ISHIHARA, T. AND A. KIGOSHI (1953) Fundamental researches on metallurgical treatment of manganese ores. I. On the equilibrium in the reduction of Mn_3O_4 with CO. *Sendai Univ. Res. Inst. Sci. Rep., Ser. A* **4-5**, 172-178.
- KIM, D. Q., Y. W., AND F. MARION (1966) Sur la détermination directe des équilibres des oxydes de manganese à haute température. *C. R. Acad. Sci. Paris, Ser. C* **262**, 756-758.
- KINGERY, W. D., J. PAPPIS, M. E. DOTY AND D. C. HILL (1959) Oxygen ion mobility in cubic $\text{Zr}_{0.85}\text{Ca}_{0.15}\text{O}_{1.85}$. *J. Amer. Cer. Soc.* **42**, 393-398.
- KIUKKOLA, K. AND C. WAGNER (1957) Measurements on galvanic cells involving solid electrolytes. *J. Electrochem. Soc.* **104**, 379-387.
- KLINGSBERG, C. AND R. ROY (1960) Solid-solid and solid-vapor reactions and a new phase in the system Mn-O. *J. Amer. Ceram. Soc.* **43**, 620-626.
- LEBLANC, M. AND G. WEHNER (1934) Beitrag zur Kenntnis der Manganoxyde. *Z. Physik. Chem.* **168A**, 59-78.
- LINDSLEY, D. H. (1963) Equilibrium relations of coexisting pairs of Fe-Ti oxides. *Carnegie Inst. Wash. Year Book* **62**, 60-66.
- MAH, A. D. (1960) Thermodynamic properties of manganese and its compounds. *U. S. Bur. Mines Rep. Invest.* **5600**, 1-34.
- MATSUSHIMA, T., AND W. J. THOBURN (1965) Application of differential thermal analysis to the dissociation of MnO_2 and Mn_2O_3 . *Can. J. Chem.* **43**, 1723-1728.
- McMURDIE, H. F., AND E. GOLOVATO (1948) Study of the modifications of manganese dioxide. *J. Res. [U.S.] Natl. Bur. Stand.* **41**, 589-600.
- , B. M. BULLIVAN AND F. A. MAUER (1950) High-temperature X-ray study of the system $\text{Fe}_3\text{O}_4\text{-Mn}_3\text{O}_4$. *J. Res. [U.S.] Natl. Bur. Stand.* **45**, 35-41.
- MOORE, T. E., M. ELLIS AND P. W. SELWOOD (1950) Solid oxides and hydroxides of manganese. *J. Amer. Chem. Soc.* **72**, 856-866.
- MUAN, ARNULF AND W. C. HAHN, JR. (1959) Some energy relations in solid state reactions involving crystalline phases of variable compositions. *J. Amer. Chem. Soc.* **63**, 1826-1830.
- OTTO, E. M. (1964) Equilibrium pressures of oxygen over $\text{Mn}_2\text{O}_3\text{-Mn}_3\text{O}_4$ at various temperatures. *J. Electrochem. Soc.* **111**, 88-92.
- RIZZO, F. E., L. R. BIDWELL, AND D. F. FRANK (1967) The standard free energy of cuprous oxide. *Trans. A.I.M.E.* **239**, 593-596.
- ROBIE, R. A. AND D. R. WALDBAUM (1968) Thermodynamic properties of minerals and related substances at 298.15°K (25.0°C) and one atmosphere (1.013 bars) pressure and at higher temperatures. *U. S. Geol. Surv. Bull.* **1259**, 1-255.
- , P. M. BETHKE, M. S. TOULMIN AND J. L. EDWARDS (1966) X-ray crystallographic data, densities, and molar volumes of minerals. *Geol. Soc. Amer. Mem.* **97**, 27-74.

- SATO, MOTOAKI (1970) An electrochemical method of oxygen fugacity control of furnace atmospheres for mineral syntheses. *Amer. Mineral.* (in press)
- SCHMAHL, N. G. AND B. STEMLER (1965) Equilibria of the Mn_2O_3 - Mn_3O_4 - O_2 systems. *J. Electrochem. Soc.* **112**, 365.
- SCHMALZRIED, H. (1962) Über Zirkondioxyd als Elektrolyt für elektrochemische Untersuchungen bei höheren Temperaturen. *Z. Elektrochem.* **66**, 572-576.
- SCHWERTFEGER, K. AND A. MUAN (1967) Equilibria in the system Fe-Mn-O involving "(Fe,Mn)O" and $(Fe,Mn)_3O_4$ solid solutions. *Trans. AIME* **239**, 1114-1119.
- SHENOUDA, F. AND S. AZIZ (1967) Equilibria and hysteresis in the system Mn_2O_3 - Mn_3O_4 - O_2 . *J. Appl. Chem.* (London), **17**, 258-262.
- SHOMATE, C. H. (1943) Heats of formation of manganomanganic oxide and manganese dioxide. *J. Amer. Chem. Soc.* **65**, 785-790.
- SOUTHARD, J. C. AND MOORE, G. E. (1942) High-temperature heat content of Mn_3O_4 , $MnSiO_3$ and Mn_3C . *J. Amer. Chem. Soc.* **64**, 1769-1770.
- AND H. C. SHOMATE (1942) Heat of formation and high-temperature heat content of manganous oxide and manganous sulfate. High temperature heat content of manganese. *J. Amer. Chem. Soc.* **64**, 1770-1774.
- THOMPSON, J. B., JR. (1955) The thermodynamic basis for the mineral facies concept. *Amer. J. Sci.* **253**, 65-103.
- ULLMANN, H. (1968) Die Sauerstoffpermeabilität von oxidischen Festelektrolyten. *Z. Physik. Chem.* **237**, 71-80.
- VAN HOOK, H. J. AND M. L. KEITH (1958) The system Fe_3O_4 - Mn_3O_4 . *Amer. Mineral.* **43**, 69-83.
- VLASOV, V. G. AND V. A. KOZLOV (1958) Kinetics of the dissociation of manganese oxides. *Zh. Fiz. Khim.* **32**, 2608-2613.
- VOELTZEL, J. AND J. MANENC (1967) Study of $(Fe,Mn)_{1-y}O$ solid solutions. *Mem. Sci. Rev. Met.* **64**, 191-194.
- WATANABE, MOTOO (1933) On the equilibrium in the reduction of nickelous oxide by carbon monoxide. *Tohoku Univ., Sci. Rep., First Ser.* **22**, 436-447.

Manuscript received, December 10, 1969; accepted for publication, January 26, 1970.

APPENDIX I

EQUATIONS BASED UPON THE IPTS 1968 (UNITS ARE ATM, °K, CALORIES)

$$\log f_{O_2}(\pm 0.04) = 9.36 - \frac{24910}{T} \quad \sigma = 0.27 \quad (2')$$

$$\log f_{O_2}(\pm 0.03) = 9.30 - \frac{24900}{T} \quad \sigma = 0.22 \quad (3')$$

$$\log f_{O_2}(\pm 0.02) = 9.36 - \frac{24930}{T} \quad \sigma = 0.25 \quad (4')$$

$$\Delta G^\circ(\pm 110) = 42.82T - 114100 \quad (5')$$

$$\log f_{O_2}(\pm 0.02) = 7.34 - \frac{9265}{T} \quad \sigma = 0.12 \quad (6')$$

$$\log f_{O_2}(\pm 0.05) = 13.38 - \frac{25680}{T} \quad \sigma = 0.24 \quad (7')$$